Transition State Chirality and Role of the Vicinal Hydroxyl in the Ribosomal Peptidyl Transferase Reaction†

Kevin S. Huang,‡,§ Nicolas Carrasco,‡ Emmanuel Pfund,|| and Scott A. Strobel*

Department of Molecular Biophysics and Biochemistry and Department of Chemistry, Yale University, 260 Whitney Avenue, New Haven, Connecticut 06520-8114

Received February 20, 2008; Revised Manuscript Received June 9, 2008

ABSTRACT: The ribosomal peptidyl transferase is a biologically essential catalyst responsible for protein synthesis. The reaction is expected to proceed through a transition state approaching tetrahedral geometry with a specific chirality. To establish that stereospecificity, we synthesized two diastereomers of a transition state inhibitor with mimics for each of the four ligands around the reactive chiral center. Preferential binding of the inhibitor that mimics a transition state with *S* chirality establishes the spatial position of the nascent peptide and the oxyanion and places the amine near the critical A76 2′-OH group on the P-site tRNA. Another inhibitor series with 2′-NH_2 and 2′-SH substitutions at the critical 2′-OH group was used to test the neutrality of the 2′-OH group as predicted if the hydroxyl functions as a proton shuttle in the transition state. The lack of significant pH-dependent binding by these inhibitors argues that the 2′-OH group remains neutral in the transition state. Both of these observations are consistent with a proton shuttle mechanism for the peptidyl transferase reaction.

The ribosome is the macromolecular machine responsible for protein synthesis (*1*). It catalyzes the peptidyl transferase reaction between two tRNA substrates: the P-site tRNA, which is linked via an ester bond to the nascent peptide chain, and the A-site tRNA, which carries the next amino acid in the polypeptide sequence. Peptide bond formation involves aminolysis of the P-site ester by nucleophilic attack of the α-amino group in the A-site. The reaction occurs within the peptidyl transferase center (PTC)[1] of the 50S ribosomal subunit where it proceeds ~10^7-fold faster than the uncatalyzed enzyme (*2*). The 2′-OH group of A76 on the P-site tRNA, which is vicinal to the O3′-linked ester, contributes ~10^6-fold to the reaction, an example of substrate-assisted catalysis (*3*). The 2′-OH group of A2451 within the rRNA also makes a significant contribution to catalysis (*4, 5*).

Like the uncatalyzed aminolysis reaction, the ribosome-promoted reaction is predicted to proceed through a chiral transition state approaching a tetrahedral geometry. Although neither the ester substrates nor the amide product is chiral, the transition state approaches sp^3 hybridization and has four different groups originating from the reactive carbon center. These include the α-amine (from the A-site tRNA), the O3′ leaving group (from the P-site tRNA), the nascent peptide, and the developing oxyanion. For an uncatalyzed reaction, the amine attacks either enantiotopic face (*re* or *si*) of the planar ester, resulting in a racemic collection of transition states (Figure 1a). However, steric features of the ribosomal active site are expected to position the amine for attack against one face, resulting in a stereospecific transition state. Establishing the chirality would define the spatial position of the oxyanion and the orientation of the amine relative to the critical 2′-OH group of A76. For the transition state with *S* chirality, the amine is near the critical A76 2′-OH group, whereas it is closer to the universally conserved A2451 in the *R* transition state. Thus, the stereospecificity of the reaction is essential for defining how the ribosome promotes peptide bond formation and the orientation of the reactive groups in the transition state.

The chirality of the peptidyl transferase transition state has been a subject of previous consideration, and arguments supporting both possibilities have been made (*6–11*). The original 50S ribosomal crystal structure predicted a transition state with *R* chirality based upon binding to the "Yarus inhibitor" (*12*), a molecule that contained the nucleic acid sequence C-C-2′-deoxy-A (CCdA) as a mimic of the P-site tRNA, puromycin (Pm) as the A-site tRNA, and an achiral phosphoramidate linkage between them to mimic the tetrahedral carbon. Although the phosphoramidate contains two equivalent oxygens, the *pro-*R_p phosphate oxygen was assigned as the oxyanion because of its proximity to A2451, which was originally predicted to play a role as the oxyanion hole (*6, 13*). Subsequent work demonstrated that the A2451 nucleobase is relatively unimportant to the reaction, which weakened the validity of this stereochemical assignment (*13–17*). Other theoretical and modeling studies also considered this question. Lim and Spirin (*7*) predicted a transition

† This work was supported by NIH Grant 54839 to S.A.S. and NIH postdoctoral fellowships to K.S.H. and N.C.

* To whom correspondence should be addressed. Phone: (203) 432-9772. Fax: (203) 432-5767. E-mail: scott.strobel@yale.edu.

‡ These authors contributed equally to this work.

§ Present address: Department of Biology and Chemistry, Azusa Pacific University, 901 E. Alosta Ave., Azusa, CA 91702-7000.

|| Present address: Laboratoire de Chimie Moléculaire et Thio-organique, UMR-CNRS 6507, Université de Caen-ENSI CAen, 6 Bd du Maréchal Juin, F 14050 Caen, France.

[1] Abbreviations: PTC, peptidyl transferase center; Pm, puromycin; hPmn, hydroxypuromycin; TS, transition state; DMTr, dimethoxytrityl; TEAA, triethylammonium acetate; CMCT, 1-cyclohexyl-3-(2-morpholinoethyl)carbodiimide metho-*p*-toluenesulfonate.

10.1021/bi800299u CCC: $40.75
Published on Web 08/02/2008

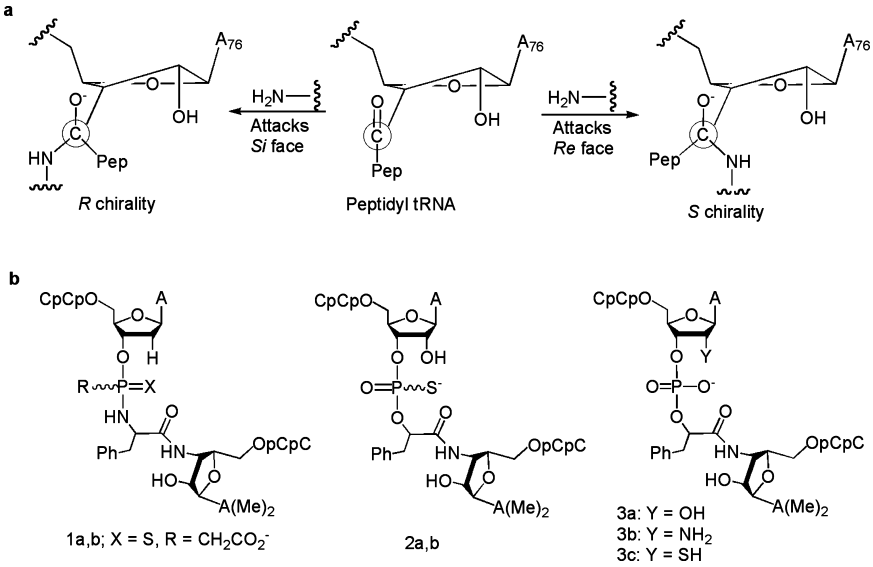

FIGURE 1: Two distinct stereoselective pathways for the peptidyl transferase reaction. (a) Nucleophilic attack by the α-amino group of the aminoacyl tRNA on the *re* face of the peptidyl tRNA proceeds to an intermediate with *S* chirality, while attack on the *si* face yields *R* chirality. For purposes of stereochemical assignment, O3′ was given priority over the carbonyl oxygen in the sp^3-hybridized intermediate shown here. (b) Transition state analogues of the peptidyl transferase reaction that include C74, C75, and A76 of the A-site and P-site tRNAs, a phenylalanine as the A-site amino acid, a chiral phosphoramidate linkage between the A-site and P-site fragments, and a methyl carboxylate that mimics the nascent peptide.

state with *R* chirality, while Das et al. (*8*) reached the opposite conclusion. Reevaluation of the 50S crystal structure led Chamberlin et al. (*9*) and Hansen et al. (*10*) to predict that the TS has *S* chirality. In the later case, this assignment was based upon a model juxtaposing the substrates in two separate A-site-bound and P-site-bound structures. To biochemically distinguish between these two mechanistic models, we designed inhibitors containing a chiral tetrahedral center and used these to determine the spatial orientation of key functional groups in the transition state.

It has also been proposed that the critical A76 2′-OH group on the P-site tRNA serves as a proton shuttle between the amino nucleophile and the O3′ leaving group (*1, 11, 18–23*). The key feature of this model is the fact that the 2′-OH group remains neutral in the transition state by accepting a proton from the amine while simultaneously donating its proton to O3′. A role as a proton shuttle was invoked in part because the pK_a values of the 2′-OH group are expected to be too high for efficient deprotonation [approximately 12 for oxyanion formation (*24–27*)] and that of the conjugated acid form is too low for deprotonation [<0 for alkyloxonium ion formation (*25*)] under physiological conditions. However, the ribosome might perturb the 2′-OH pK_a in the transition state to facilitate proton transfer. To provide biochemical evidence of the role of the 2′-OH group as a proton shuttle, we investigated the ionization state of this group by measuring the binding affinity of a series of peptidyl transferase inhibitors containing 2′-OH, 2′-NH_2, and 2′-SH substitutions as a function of pH. On the basis of the results that were obtained, we present new insights into how the ribosome might catalyze peptide bond formation using a proton shuttle mechanism insofar as the inhibitors used accurately mimic the transition state of peptide bond formation.

MATERIALS AND METHODS

Inhibitor Synthesis. A racemic mixture of inhibitors **1a** and **1b** was prepared by solid phase chemical synthesis based upon the method described previously (*28, 29*). The polymer-bound hydroxypuromycin (hPm) was coupled with 5′-DMTr-adenosine-3′-(carbomethoxy-1,1-dimethyl-2-cyanoethyl)phosphinoamidite (MetaSense Technologies, LLC) followed by sulfurization with 3*H*-1,2-benzodithiole-3-one-1,1-dioxide (Glen Research) to produce a racemic mixture of the phosphonocarboxylate dinucleotide on a solid support. Two rounds of C phosphoramidite coupling, acid deprotection, and cleavage from the solid support afforded a racemic mixture of the inhibitors. The two diastereomers were then separated by HPLC using a C18 reversed phase Zorbax column (Hewlett-Packard) and a 50 mM triethylammonium acetate (TEAA, pH 7.0)/acetonitrile gradient. The identity of the compounds was confirmed by mass spectrometry, and the absolute stereochemistry was established by X-ray crystallography. See the Supporting Information for detailed information.

A racemic mixture of inhibitors **2a** and **2b** was prepared in similar fashion using 5′-DMTr-*N*-PAC-adenosine phosphoramidite (Glen Research) in place of the carbomethoxy-derivatized phosphinoamidite. The two diastereomers were also separated by HPLC as described above.

Inhibitors **3a**, **3b**, and **3c** containing 2′-OH, 2′-NH_2, and 2′-SH substitutions, respectively, were prepared by solid phase chemical synthesis as previously described (*28, 30*) except adenosine synthons containing appropriately protected 2′-NH_2 or 2′-SH groups were used in the initial coupling to hydroxypuromycin. Inhibitor **3b** was prepared by coupling the 4-*N*-benzoyl-5′-*O*-(BzH)-2′-deoxy-2′-(tritylamino)adenosin-3′-yl β-cyanoethyl *N*,*N*-diisopropylphosphoramidite, while **3c** was prepared by coupling the 4-*N*-benzoyl-5′-O-(dimethoxytrityl)-2′-deoxy-2′-(tritylthio)adenosin-3′-yl β-cyanoethyl *N*,*N*-diisopropylphosphoramidite. After removal from the solid support, the 2′-trityl protecting group was removed using published procedures (*31*).

Measurement of Inhibitor Binding Affinities. The binding affinities of inhibitors **1a,b** and **2a,b** for the peptidyl

transferase center were determined by chemical footprinting of residue U2585 with 1-cyclohexyl-3-(2-morpholinoethyl)-carbodiimide metho-*p*-toluenesulfonate (CMCT) (*28, 32–34*). The extent of CMCT modification as a function of analogue concentration was determined by reverse transcription, and the resulting data were used to calculate the dissociation constants (K_d) using the equation $I = I_{sat} + (I_0 - I_{sat})/(1 + [\text{inhibitor}]/K_d)$, where I is the band intensity of the modified residue, I_{sat} is the band intensity of the modified residue when inhibitor is saturating, and I_0 is the band intensity of the modified residue in the absence of inhibitor. All band intensities were normalized relative to CMCT-dependent bands for gel loading and for extent of CMCT reactivity with the 50S rRNA. To test for thiophilic metal-dependent binding to the PTC, 1 mM Mn^{2+}, 100 μM Zn^{2+}, or 100 μM Cd^{2+} was added to the ribosomes prior to addition of inhibitors **2a** and **2b**.

Binding affinities of inhibitors **3a**−**c** were measured as a function of pH by chemical footprinting using dimethyl sulfate (DMS) modification at A2602 followed by primer extension (*13, 33, 34*). Modification at A2602 was monitored as a function of pH by reverse transcription, and the binding constants of the inhibitors were determined as described above. A single three-buffer system (EPPS/MOPS/MES) was used to reach the pHs across this range. Methanol (33%) was added to increase the binding affinity of inhibitor **3c** within a range that could be measured by this assay. See the Supporting Information for detailed information.

RESULTS

This study evaluates several features of the peptidyl transferase transition state using the relative binding affinity of various TS analogues. The expectation is that the analogue that most closely mimics the TS will have the highest binding affinity.

To define the chirality of the PT reaction, we synthesized an expanded version of the Yarus inhibitor (*32*) containing a phosphoramidate linkage between the two tRNA segments (**1**, Figure 1b). Unlike the Yarus inhibitor, which was achiral at the tetrahedral center, inhibitor **1** has both an *R* and an *S* diastereomer. In this molecule, CCdA represents the P-site tRNA, CChPm is the aminoacyl tRNA in the A-site (hPm-hydroxypuromycin), the sulfur is designed to mimic the ionized oxyanion, and the methylcarboxylate is a short representation of the nascent peptide. Steric and electrostatic features within the chiral peptidyl transferase center should result in preferential binding of one inhibitor over the other. Thus, the diastereomer with the highest binding affinity for the ribosome is the one that most closely matches the transition state. Because the atomic priority is reversed for a sulfur-containing mimic relative to the natural oxygen-containing TS, the stereochemical assignment of **1a** and **1b** is correspondingly reversed. As a result, and to avoid confusion, we made the stereochemical assignment on the basis of the atomic priority of the ligands in the proposed intermediates (Figure 1a).

The relative binding affinities of the two diastereomers were measured in parallel by CMCT modification at U2585 within the 23S rRNA (Figure 2). The inhibitor that mimics the transition state with an *S* chirality bound with an affinity of 77 ± 15 nM, while the other diastereomer bound 20-fold

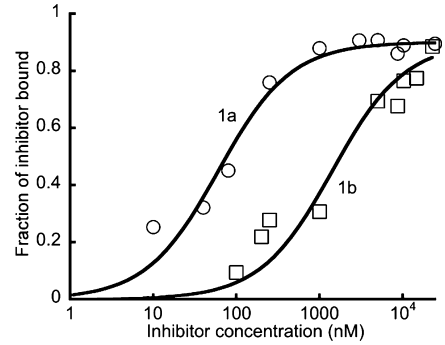

FIGURE 2: Relative affinities of chiral inhibitors **1a** and **1b**. Affinities were measured by CMCT footprinting at U2585 in domain V of the peptidyl transferase center. The fraction of inhibitor bound as a function of inhibitor concentration (log scale) was used to determine the relative dissociation constants (K_d) of the two inhibitors.

weaker with an affinity of 1500 ± 350 nM. Even though the peptide mimic in this inhibitor molecule was relatively small, the ~1.8 kcal/mol difference in affinity demonstrates that the ribosome has a clear stereospecificity for an *S* transition state. This quantitative characterization of inhibitor affinities agrees with qualitative observations made in a previous crystallographic study involving a racemic mixture of these two inhibitors. In that case, the racemic mixtures were soaked into the ribosomal crystals, but in the resulting $F_o - F_c$ electron density map, only density for the inhibitor that mimics the transition state with an *S* chirality appeared in the PTC (*11*). Thus, a transition state with *S* chirality places the oxyanion away from the A2451 N3 atom, as proposed in the original 50S structure (*35*), and oriented toward a small cavity between the A-site and P-site tRNAs (*11*).

To test the possibility that a metal ion might bind to this cavity and stabilize the oxyanion, we used a second diastereomeric pair of inhibitors (**2a** and **2b**, Figure 1b) containing a sulfur and an oxygen to mimic the oxyanion and the nascent peptide, respectively. If there is a metal−oxyanion interaction, then the sulfur substitution would be expected to negatively affect the affinity of the inhibitor (*36*). We observed that both diastereomers bound with equal affinity (220 ± 20 and 250 ± 70 nm, respectively). Equivalent binding affinities between diastereomers **2a** and **2b** argue that differential binding by inhibitors **1a** and **1b** results primarily from a preferred orientation for the methyl carboxylate mimic of the nascent peptide. The ribosome shows no preference for an oxygen or a sulfur in the position of the oxyanion. To explore this further, we next tested if addition of thiophilic metal ions would selectively increase the affinity of either inhibitor for the active site. Binding constants of both inhibitors were measured in the presence of three different thiophilic metal ions (Mn^{2+}, Cd^{2+}, and Zn^{2+}). In each case, there was no appreciable change in the affinity of either inhibitor (data not shown). The indistinguishable difference between oxygen or sulfur as the oxyanion mimic and the absence of a metal specificity switch are consistent with the crystallographic observation that the "oxyanion hole" is occupied by a water molecule (*11*).

A transition state with *S* chirality places the nucleophilic α-amine within hydrogen bonding distance of the critical A76 2′-OH group on the P-site tRNA (*37*). To explore

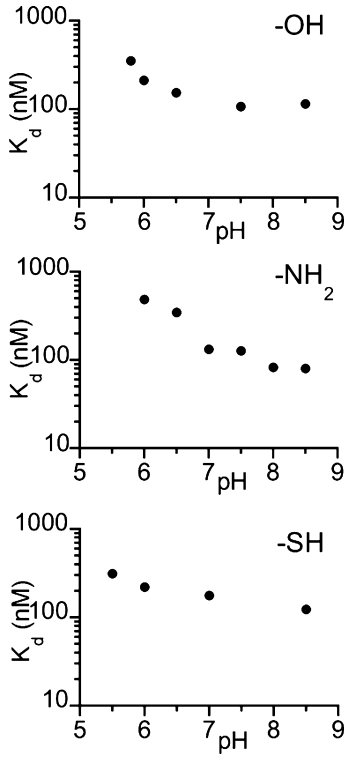

FIGURE 3: pH dependence of the binding affinities of the 2′-OH, -NH_2, and -SH inhibitors (**3a**−**c**, respectively) as measured by the extent of DMS modification at A2602.

ionization of the 2′-OH group, we prepared inhibitors with 2′-OH, 2′-NH_2, and 2′-SH substitutions (**3a**−**c**, respectively, Figure 1b) at the P-site A76 position and measured their binding affinity for the ribosome by dimethyl sulfate (DMS) modification at A2602 in the 23S rRNA. Unlike CMCT, which is unreactive below pH 7, the extent of DMS modification is largely pH-independent from pH 5.5 to 8.5 (see the Supporting Information for detailed information). The pK_a for protonation of the amine is expected to be approximately 6 (*38, 39*), while the pK_a for deprotonation of the sulfhydryl is approximately 7 (*40, 41*). Selective binding of either inhibitor as a function of pH (the NH_3^+ forms at low pH or the S^- forms at high pH) would provide evidence that the ribosome stabilizes an ionized form of the A76 2′-OH group.

We first determined the pH dependence for binding by the 2′-OH inhibitor (**3a**) as a benchmark for comparison. At pH 7.5 and 8.5, the inhibitor bound with an affinity of 110 ± 10 nM (Figure 3). The affinity decreased, but only slightly (3-fold), at low pH (5.8), a result generally consistent with the pH independence of Yarus inhibitor binding reported previously (*13*). If the ribosome stabilizes the protonated form of the hydroxyl in the transition state, then the 2′-NH_2 inhibitor (**3b**) should bind tighter at acidic pH, where the elevated pK_a of the amine would significantly populate the ammonium form. Instead, we found that the binding profile was equivalent to that of the 2′-OH inhibitor. The affinity was slightly weaker (4-fold) at pH 6 than at pH 7. Deprotonation of the hydroxyl group was also explored using the 2′-SH-substituted inhibitor (**3c**). If the ribosome stabilizes a 2′-oxyanion in the transition state, then the 2′-SH inhibitor should bind tighter in its deprotonated form at higher pH. The overall affinity of **3c** was substantially lower than that of **3a** and **3b**. To measure the affinity, it was necessary to add methanol to the reaction mixture. Experiments on the 2′-OH inhibitor showed that methanol does not affect the pH dependence of the binding affinity (data not shown). Thus, while the absolute affinities of the three inhibitors cannot be directly compared, the relative changes in affinity as a function of pH are relevant. Inhibitor **3c** exhibited the same modest 3-fold increase in affinity between pH 5.5 and 8.5 that was observed for **3a** and **3b**. The lack of a substantial change in affinity for any of the inhibitors as a function of pH argues that the ribosome does not preferentially bind a transition state analogue with either a positively charged or a negatively charged group at the 2′-OH position. Because preferential binding would be an indication of the substantial energy needed to perturb the 2′-OH pK_a for ionization, these data argue that the 2′-OH group remains neutral in the transition state.

DISCUSSION

The mechanism of peptide bond formation remains an area of active investigation. Our results provide valuable spatial and chemical information needed to understand how the ribosome catalyzes this essential biological reaction. A transition state with *S* chirality establishes the orientation of the nucleophilic amine, the nascent peptide, and the oxyanion within the active site. This stereospecificity means the nascent peptide is near A2451, the developing oxyanion points into a cleft formed between the ends of the A-site and P-site tRNAs, and the α-amino group is near the 2′-OH group of A76. In this orientation, the critical 2′-OH group is located

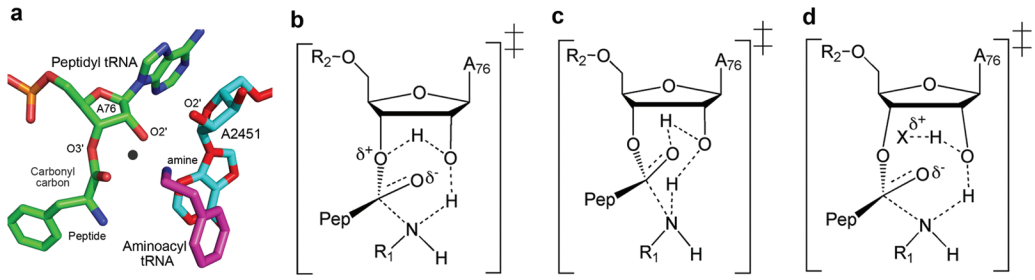

FIGURE 4: Possible mechanisms of peptide bond formation catalyzed by the ribosome that employ the O2′ atom of peptidyl tRNA A76 as a proton shuttle. (a) View of A76 O2′ in relation to other functional groups in the ground state crystal structure (created from Protein Data Bank entry 1VQN). The water molecule is represented by the dark sphere. (b) Enforced concerted mechanism involving partial proton transfer onto O3′. (c) Stepwise mechanism involving partial proton transfer onto the carbonyl oxygen. (d) Partial proton transfer to a ribosomal group (represented by X) such as an ordered water molecule or O2′ of A2451. In all cases, the nitrogen and O2′ atoms are neutral in the transition state. Concerted bond making and bond breaking are shown by dashed bonds, while the stereochemistry is depicted by wedged and hashed wedged bonds. R_1 = aminoacyl tRNA. R_2 = peptidyl tRNA. Pep = nascent peptide.

between the nucleophile, the carbonyl oxygen, and the O3′ leaving group of the transition state reaction (Figure 4a).

These results are complemented by the recent determination of the Brønsted coefficient of the nucleophile (β_{nuc}) for both the modified 50S fragment reaction and the 70S initiation complex reaction. In both cases, β_{nuc} was close to zero (*42, 43*). β_{nuc} measures the change in charge on the α-amine between the ground state and the transition state. A value near zero demonstrates that the amine remains neutral in the transition state, while a value close to one would have indicated that it is positively charged. These results were interpreted to mean that the extent of N−C bond formation is commensurate with the degree of amine deprotonation in the transition state. With the exception of a very early transition state in which there is no N−C bond formation, a mechanism inconsistent with the tight and stereoselective binding affinity of these inhibitors, a β_{nuc} of 0 argues that the amine is partially deprotonated in the transition state. The A76 2′-OH group on the P-site tRNA is in the right position and is sufficiently catalytically important to play this role; however, the binding affinity data of the 2′-substituted inhibitors indicate that the hydroxyl remains neutral. Furthermore, analysis of the 70S ribosome reaction with full-sized tRNAs demonstrated that the reaction is not pH-dependent and is unlikely to involve the action of a general base (*44*). Thus, if the 2′-OH group partially deprotonates the amine as the N−C bond forms, it must simultaneously donate its proton a commensurate degree to another group in the active site to remain neutral. This is the hallmark prediction of the proton shuttle mechanism (*18, 22, 23, 37, 45–49*) for peptidyl transfer, though it differs in a key detail from that of Schmeing et al., in that the α-amino group also remains uncharged in the transition state.

The recipient of the proton shuttled through the 2′-OH group has not been established by any of the experiments reported to date, but three possibilities are apparent. The first is partial protonation of O3′, which would activate the leaving group (Figure 4b). This could occur either prior to or simultaneous with C−O3′ bond breakage, resulting in an enforced−concerted (*50*) or a fully concerted reaction mechanism (*18*), respectively. The second possibility, which is based upon geometric considerations and molecular dynamics simulations (*49*), is partial proton transfer to the carbonyl oxygen (Figure 4c). O2′ is positioned within hydrogen bonding distance of the carbonyl oxygen (3.36 Å) in the ground state structure of the A-site- and P-site-bound substrates (*37*). Protonation of the carbonyl oxygen would neutralize the negative charge developing on the oxyanion, resulting in a neutral intermediate. Minimal charge development on the carbonyl oxygen would explain how a water molecule could be sufficient to occupy the oxyanion hole. As the intermediate is resolved into products, the proton could then be transferred to the O3′ leaving group. The third possibility is partial proton transfer to a functional group within the ribosome. Two candidates are a water molecule that forms hydrogen bonds to both O2′ and O3′ of A76, or O2′ of A2451, which is also within hydrogen bonding distance of A76 O2′ (2.98 Å) and has been shown to be important for peptide bond formation (Figure 4a,d) (*4, 5, 37*).

In summary, these data define the transition state chirality and charge state of the P-site A76 2′-OH group within the peptidyl transferase center. The binding affinity data of the transition state inhibitors demonstrate that the reaction proceeds via a transition state with *S* chirality, no divalent metal ions appear to stabilize the developing oxyanion, and the vicinal 2′-OH group remains neutral. Although these findings cannot fully distinguish between alternative proton shuttle mechanisms, they establish important criteria that must be met in mechanistic considerations of this reaction.

ACKNOWLEDGMENT

We thank J. Kavran and T. A. Steitz for helping to establish the absolute stereochemistry of the purified inhibitor by X-ray crystallography, O. Fedorova and D. Kitchen for technical assistance in solid phase synthesis, and D. Kingery, J. Cochrane, and J. Weinger for helpful discussions.

SUPPORTING INFORMATION AVAILABLE

Detailed synthetic procedures, including chemical compound characterization and chemical footprinting. This material is available free of charge via the Internet at http://pubs.acs.org.

REFERENCES

1. Beringer, M., and Rodnina, M. V. (2007) The ribosomal peptidyl transferase. *Mol. Cell 26*, 311–321.
2. Sievers, A., Beringer, M., Rodnina, M. V., and Wolfenden, R. (2004) The ribosome as an entropy trap. *Proc. Natl. Acad. Sci. U.S.A. 101*, 7897–7901.
3. Weinger, J. S., Parnell, K. M., Dorner, S., Green, R., and Strobel, S. A. (2004) Substrate-assisted catalysis of peptide bond formation by the ribosome. *Nat. Struct. Mol. Biol. 11*, 1101–1106.
4. Erlacher, M. D., Lang, K., Wotzel, B., Rieder, R., Micura, R., and Polacek, N. (2006) Efficient ribosomal peptidyl transfer critically relies on the presence of the ribose 2′-OH at A2451 of 23S rRNA. *J. Am. Chem. Soc. 128*, 4453–4459.
5. Erlacher, M. D., Lang, K., Shankaran, N., Wotzel, B., Huttenhofer, A., Micura, R., Mankin, A. S., and Polacek, N. (2005) Chemical engineering of the peptidyl transferase center reveals an important role of the 2′-hydroxyl group of A2451. *Nucleic Acids Res. 33*, 1618–1627.
6. Nissen, P., Hansen, J., Ban, N., Moore, P. B., and Steitz, T. A. (2000) The structural basis of ribosome activity in peptide bond synthesis. *Science 289*, 920–930.
7. Lim, V. I., and Spirin, A. S. (1986) Stereochemical analysis of ribosomal transpeptidation. Conformation of nascent peptide. *J. Mol. Biol. 188*, 565–574.
8. Das, G. K., Bhattacharyya, D., and Burma, D. P. (1999) A possible mechanism of peptide bond formation on ribosome without mediation of peptidyl transferase. *J. Theor. Biol. 200*, 193–205.
9. Chamberlin, S. I., Merino, E. J., and Weeks, K. M. (2002) Catalysis of amide synthesis by RNA phosphodiester and hydroxyl groups. *Proc. Natl. Acad. Sci. U.S.A. 99*, 14688–14693.
10. Hansen, J. L., Schmeing, T. M., Moore, P. B., and Steitz, T. A. (2002) Structural insights into peptide bond formation. *Proc. Natl. Acad. Sci. U.S.A. 99*, 11670–11675.
11. Schmeing, T. M., Huang, K. S., Kitchen, D. E., Strobel, S. A., and Steitz, T. A. (2005) Structural insights into the roles of water and the 2′ hydroxyl of the P site tRNA in the peptidyl transferase reaction. *Mol. Cell 20*, 437–448.
12. Welch, M., Chastang, J., and Yarus, M. (1995) An inhibitor of ribosomal peptidyl transferase using transition-state analogy. *Biochemistry 34*, 385–390.
13. Parnell, K. M., Seila, A. C., and Strobel, S. A. (2002) Evidence against stabilization of the transition state oxyanion by a pK_a-perturbed RNA base in the peptidyl transferase center. *Proc. Natl. Acad. Sci. U.S.A. 99*, 11658–11663.
14. Polacek, N., Gaynor, M., Yassin, A., and Mankin, A. S. (2001) Ribosomal peptidyl transferase can withstand mutations at the putative catalytic nucleotide. *Nature 411*, 498–501.
15. Youngman, E. M., Brunelle, J. L., Kochaniak, A. B., and Green, R. (2004) The active site of the ribosome is composed of two layers

of conserved nucleotides with distinct roles in peptide bond formation and peptide release. *Cell 117*, 589–599.
16. Thompson, J., Kim, D. F., O'Connor, M., Lieberman, K. R., Bayfield, M. A., Gregory, S. T., Green, R., Noller, H. F., and Dahlberg, A. E. (2001) Analysis of mutations at residues A2451 and G2447 of 23S rRNA in the peptidyltransferase active site of the 50S ribosomal subunit. *Proc. Natl. Acad. Sci. U.S.A. 98*, 9002–9007.
17. Beringer, M., Bruell, C., Xiong, L., Pfister, P., Bieling, P., Katunin, V. I., Mankin, A. S., Bottger, E. C., and Rodnina, M. V. (2005) Essential mechanisms in the catalysis of peptide bond formation on the ribosome. *J. Biol. Chem. 280*, 36065–36072.
18. Dorner, S., Polacek, N., Schulmeister, U., Panuschka, C., and Barta, A. (2002) Molecular aspects of the ribosomal peptidyl transferase. *Biochem. Soc. Trans. 30*, 1131–1136.
19. Trobro, S., and Aqvist, J. (2005) Mechanism of peptide bond synthesis on the ribosome. *Proc. Natl. Acad. Sci. U.S.A. 102*, 12395–12400.
20. Trobro, S., and Aqvist, J. (2006) Analysis of predictions for the catalytic mechanism of ribosomal peptidyl transfer. *Biochemistry 45*, 7049–7056.
21. Rangelov, M. A., Vayssilov, G. N., Yomtova, V. M., and Petkov, D. D. (2006) The syn-oriented 2-OH provides a favorable proton transfer geometry in 1,2-diol monoester aminolysis: Implications for the ribosome mechanism. *J. Am. Chem. Soc. 128*, 4964–4965.
22. Bayryamov, S. G., Rangelov, M. A., Mladjov, A. P., Yomtova, V. M., and Petkov, D. D. (2007) Unambiguous evidence for efficient chemical catalysis of adenosine ester aminolysis by its 2′/3′-OH. *J. Am. Chem. Soc. 129*, 5790–5791.
23. Changalov, M. M., and Petkov, D. D. (2007) Linear free energy relationships and kinetic isotope effects reveal the chemistry of the Ado 2′-OH group. *Tetrahedron Lett. 48*, 2381–2384.
24. Bevilacqua, P. C., Brown, T. S., Nakano, S., and Yajima, R. (2004) Catalytic roles for proton transfer and protonation in ribozymes. *Biopolymers 73*, 90–109.
25. Acharya, S., Foldesi, A., and Chattopadhya, J. (2003) The pKa of the internucleotidic 2′-hydroxyl group in diribonucleoside (3′→5′) monophosphate. *J. Org. Chem. 68*, 1906–1910.
26. Lyne, P. D., and Karplus, M. (2000) Determination of the pKa of the 2′-hydroxyl group of a phosphorylated ribose: Implications for the mechanism of hammerhead ribozyme catalysis. *J. Am. Chem. Soc. 122*, 166–167.
27. Li, Y., and Breaker, B. B. (1999) Kinetics of RNA degradation by specific base catalysis of transesterification involving 2′-hydroxyl group. *J. Am. Chem. Soc. 121*, 5364–5372.
28. Huang, K. S., Weinger, J. S., Butler, E. B., and Strobel, S. A. (2006) Regiospecificity of the peptidyl tRNA ester within the ribosomal P site. *J. Am. Chem. Soc. 128*, 3108–3109.
29. Weinger, J. S., Kitchen, D., Scaringe, S. A., Strobel, S. A., and Muth, G. W. (2004) Solid phase synthesis and binding affinity of peptidyl transferase transition state mimics containing 2′-OH at P-site position A76. *Nucleic Acids Res. 32*, 1502–1511.
30. Porcher, S., Meyyappan, M., and Pitsch, S. (2005) Spontaneous aminoacylation of a RNA sequence containing a 3′-terminal 2′-thioadenosine. *Helv. Chim. Acta 88*, 2897–2909.
31. Hamm, M. L., and Piccirilli, J. A. (1997) Incorporation of 2′-deoxy-2′-mercaptocytidine into oligonucleotides via phosphoramidite chemistry. *J. Org. Chem. 62*, 3415–3420.
32. Welch, M., Chastang, J., and Yarus, M. (1995) An inhibitor of ribosomal peptidyl transferase using transition-state analogy. *Biochemistry 34*, 385–390.
33. Moazed, D., Stern, S., and Noller, H. F. (1986) Rapid chemical probing of conformation in 16 S ribosomal RNA and 30 S ribosomal subunits using primer extension. *J. Mol. Biol. 187*, 399–416.
34. Stern, S., Moazed, D., and Noller, H. F. (1988) Structural analysis of RNA using chemical and enzymatic probing monitored by primer extension. *Methods Enzymol. 164*, 481–489.
35. Nissen, P., Hansen, J., Ban, N., Moore, P. B., and Steitz, T. A. (2000) The structural basis of ribosome activity in peptide bond synthesis. *Science 289*, 920–930.
36. Pecoraro, V. L., Hermes, J. D., and Cleland, W. W. (1984) Stability constants of Mg^{2+} and Cd^{2+} complexes of adenine nucleotides and thionucleotides and rate constants for formation and dissociation of MgATP and MgADP. *Biochemistry 23*, 5262–5271.
37. Schmeing, T. M., Huang, K. S., Kitchen, D. E., Strobel, S. A., and Steitz, T. A. (2005) Structural insights into the roles of water and the 2′ hydroxyl of the P site tRNA in the peptidyl transferase reaction. *Mol. Cell 20*, 437–448.
38. Shan, S. O., and Herschlag, D. (1999) Probing the role of metal ions in RNA catalysis: Kinetic and thermodynamic characterization of a metal ion interaction with the 2′-moiety of the guanosine nucleophile in the *Tetrahymena* group I ribozyme. *Biochemistry 38*, 10958–10975.
39. Aurup, H., Tuschl, T., Benseler, F., Ludwig, J., and Eckstein, F. (1994) Oligonucleotide duplexes containing 2′-amino-2′-deoxycytidines: Thermal stability and chemical reactivity. *Nucleic Acids Res. 22*, 20–24.
40. Dantzman, C., and Kiessling, L. (1996) Reactivity of a 2′-thio nucleotide analog. *J. Am. Chem. Soc. 118*, 11715–11719.
41. Patel, A., Schrier, W., and Nagyvary, J. (1980) Synthesis and properties of 2′-deoxy-2′-thiocytidine. *J. Org. Chem. 45*, 4830–4834.
42. Okuda, K., Seila, A. C., and Strobel, S. A. (2005) Uncovering the enzymatic pKa of the ribosomal peptidyl transferase reaction utilizing a fluorinated puromycin derivative. *Biochemistry 44*, 6675–6684.
43. Kingery, D., Pfund, E., Voorhees, R. M., Okuda, K., Wohgemuth, I., Kitchen, D. E., Rodnina, M. V., and Strobel, S. A. (2008) An uncharged amine in the transition state of the ribosomal peptidyl transfer reaction. *Chem. Biol. 15*, 493–500.
44. Bieling, P., Beringer, M., Adio, S., and Rodnina, M. V. (2006) Peptide bond formation does not involve acid-base catalysis by ribosomal residues. *Nat. Struct. Mol. Biol. 13*, 423–428.
45. Weinger, J. S., Parnell, K. M., Dorner, S., Green, R., and Strobel, S. A. (2004) Substrate-assisted catalysis of peptide bond formation by the ribosome. *Nat. Struct. Mol. Biol. 11*, 1101–1106.
46. Beringer, M., Bruell, C., Xiong, L., Pfister, P., Bieling, P., Katunin, V. I., Mankin, A. S., Bottger, E. C., and Rodnina, M. V. (2005) Essential mechanisms in the catalysis of peptide bond formation on the ribosome. *J. Biol. Chem. 280*, 36065–36072.
47. Trobro, S., and Aqvist, J. (2005) Mechanism of peptide bond synthesis on the ribosome. *Proc. Natl. Acad. Sci. U.S.A. 102*, 12395–12400.
48. Trobro, S., and Aqvist, J. (2006) Analysis of predictions for the catalytic mechanism of ribosomal peptidyl transfer. *Biochemistry 45*, 7049–7056.
49. Rangelov, M. A., Vayssilov, G. N., Yomtova, V. M., and Petkov, D. D. (2006) The syn-oriented 2-OH provides a favorable proton transfer geometry in 1,2-diol monoester aminolysis: Implications for the ribosome mechanism. *J. Am. Chem. Soc. 128*, 4964–4965.
50. Jencks, W. P. (1980) When is an intermediate not an intermediate? Enforced Mechanisms of general acid-base catalyzed, carbocation, carbanion, and ligand exchange reaction. *Acc. Chem. Res. 13*, 161–169.

BI800299U